Journal of Applied Food Technology

Home page: https://ejournal2.undip.ac.id/index.php/jaft

Green Chitosan Extraction from Vannamei Shrimp Shell Waste Using Natural Organic Acids for Food Biopolymer Applications

Kartika Gemma Pravitri*, Muhammad Nizhar Naufali, Keisha Zahrani Widiyastuti

Departement of Food Technology, Universitas Bumigora, Jl. Ismail Marzuki No. 22, Cilinaya, Cakranegara, Mataram, Nusa Tenggara Barat, Indonesia, 83121

*Corresponding author (kartika@universitasbumigora.ac.id)

Abstract

Vannamei shrimp shell waste represents a promising renewable resource for sustainable chitosan production in food biopolymer applications. This study aimed to optimize the eco-friendly extraction of chitosan from Vannamei shrimp shell waste using a combination of *Averrhoa bilimbi* extract and citric acid as natural organic acids during the demineralization process. Response Surface Methodology (RSM) with Central Composite Design (CCD) was employed to evaluate the effects of citric acid concentration and soaking time on ash content reduction. The optimum extraction condition was obtained at 25.260% citric acid concentration and 100.470 minutes soaking time, resulting in chitosan with 7.464% ash content. The optimized chitosan exhibited moisture, protein, lipid, and carbohydrate contents of 11.52%, 0.49%, 0.06%, and 80.45%, respectively, with a moderate degree of deacetylation (65.98%). FTIR analysis confirmed the presence of characteristic chitosan functional groups, including O–H, N–H, C–H, and C–O vibrations, indicating successful deacetylation and chitosan formation. Morphological analysis using Scanning Electron Microscopy (SEM) revealed a porous and interconnected surface structure compared to commercial chitosan. In addition, the optimized chitosan showed lower ash and protein contents than commercial chitosan, indicating effective mineral and protein removal during extraction. These findings demonstrate that natural organic acids can serve as environmentally friendly alternatives to mineral acids for chitosan extraction and highlight their potential application in biodegradable food packaging and edible coating applications.

Article information:
Received: 20 May 2026
Accepted: 17 July 2026
Available online: 18 July 2026

Keywords:
eco-friendly extraction
food biopolymer
natural organic acids
shrimp shell waste
sustainable food processing

doi: 10.17728/jaft.32279

Introduction

Vannamei shrimp is one of the main fishery commodities in North Lombok Regency, West Nusa Tenggara (Hilyana et al., 2023). During its growth, shrimp molt, producing high amounts of waste that can contribute to environmental pollution if not properly managed (Hosney et al., 2022). In addition, the shrimp shell consists of a biopolymer with significant commercial value known as chitin (15-20%) (Iber et al., 2022) which can be extracted into chitosan to be used as a food preservative (Sheikh et al., 2021), antibacterial agent (Affes et al., 2024), and raw material for edible film production (Sarofa et al., 2025).

Chitosan is a natural polysaccharide. (Wang and Zhuang, 2022) and is classified as a polycationic polysaccharide biopolymer derived from chitin, consisting of N-acetyl-D-glucosamine units linked by β (1,4) glycosidic bonds. The extraction of chitosan from chitin involves three stages, which are deproteination, demineralization, and deacetylation (Artilia et al., 2023). Demineralization is performed to remove minerals, particularly calcium carbonate, to enhance the purity of chitosan (Katsoulis and Rovoli, 2021). In general, this process uses hydrochloric acid (HCl) since it is proven to be highly effective in reducing mineral content (Hosney et al., 2022). However, the use of strong acids poses risks of negative impacts on the environment and health, which requires special handling (Tkachenko et al., 2022). Additionally, hydrochloric acid is not easily accessible to the general public. Therefore, an eco-friendly alternative is necessary, such as using organic acids to align with green industry principles in the chitosan demineralization process.

Organic acids are commonly weak acids that are not fully dissociated in water and have a molecular structure containing a carboxyl group (single bond –COOH) (Zhang et al., 2025). Organic acids can be used as preservatives and solvents in chitosan demineralization (El-Araby et al., 2022), offering an eco-friendly and low-cost alternative to strong acids like hydrochloric acid (HCl) (Pérez et al., 2022). Organic acids are of several types, including acetic acid, oxalic acid, ascorbic acid, and citric acid (Zamani Mazdeh et al., 2025). Some of these acids are known to be present

in Averrhoa bilimbi, namely citric acid and oxalic acid (Hazmi et al., 2024). These have previously been utilized in gelatin extraction (Syandri et al., 2025).

In the research on chitosan extraction, the selection of acid type and demineralization process conditions can affect the quality of the resulting chitosan. Previous studies have generally used inorganic acids such as HCl (Espinosa-Solís et al., 2024) or a single type of organic acid, such as acetic acid (Ozel and Elibol, 2024), lactic acid(El-Araby et al., 2022), and citric acid (Hahn et al., 2024). However, the use of acids derived from natural sources has not been extensively explored, particularly the use of *Averrhoa bilimbi* extract (Pravitri et al., 2025) have been explored the use of *Averrhoa bilimbi* extract as a natural reagent in the chitosan demineralization process has been explored; however, the mineral reduction based on ash content remains relatively high, necessitating further optimization. It was found that using other types of acid, like citric acid, can lower ash content to 0.02% and increase the degree of deacetylation to 85.2% (Psarianos et al., 2022). Therefore, the combination of *Averrhoa bilimbi* extract and citric acid has the potential to enhance the efficiency of chitosan demineralization (Pravitri et al., 2025). Additionally, according to research (Septiani and Supriyo, 2022), The duration of soaking also affects the efficiency of the chitosan demineralization process. Based on the previous background, information regarding the conditions of the demineralization process using organic acid combinations in shrimp shell chitosan extraction is still very limited, particularly the utilization of *Averrhoa bilimbi* extract as a natural reagent and its optimization. The addition of other organic acids, such as citric acid, is expected to enhance the efficiency of the demineralization process in chitosan extraction. Therefore, optimization of the concentration of citric acid addition and the duration of the soaking process is necessary. Furthermore, some of these organic acids are naturally present in *Averrhoa bilimbi*, indicating its potential as an environmentally friendly demineralization agent for chitosan extraction. However, previous studies have mainly focused on single-organic-acid systems, while limited studies have investigated the optimization of combined natural organic acid systems for eco-friendly chitosan extraction. Therefore, the novelty of this study lies in the optimization of a combined natural organic acid system consisting of *Averrhoa bilimbi* extract and citric acid to support eco-friendly chitosan extraction for food biopolymer applications.

This study aimed to optimize eco-friendly chitosan extraction from Vannamei shrimp shell waste using combined natural organic acids through Response Surface Methodology (RSM). Specifically, a Central Composite Design (CCD) approach within RSM will be employed to identify the optimal concentration of citric acid addition and soaking time, as CCD effectively models linear, interaction, and quadratic effects of process variables and provides a reliable prediction of optimum conditions for process optimization. Ash content serves as the primary response parameter for process optimizations, as it reflects the overall mineral content remaining after demineralization and enables the prediction of the optimal process conditions to achieve the lowest residual mineral content. Since ash content represents total mineral residues rather than specific minerals, the optimized chitosan will subsequently undergo a verification stage and further characterization, including the analysis of specific mineral contents to evaluate the effectiveness of calcium carbonate removal. The optimized chitosan will then be compared with commercially available chitosan. This research is expected to offer an environmentally friendly and easily adaptable alternative extraction method, aligning with green industry principles.

Materials and Methods

Materials

The tools that need to be prepared are a cabinet dryer (Memmert, Germany) , blender (Miyako, Indonesia), slow juicer (Bolde, Indonesia), sieve, glass funnel (Iwaki, Japan), measuring flask, filter cloth (Indonesia), measuring pipette, stirring rod, pH meter (China), filt, digital scale (Camry, China), and erlenmeyer flask (Iwaki, Japan). Meanwhile, the materials used are shrimp shell waste from North Lombok Regency, NaOH (Merck, Germany), distilled water, citric acid (Merck, Germany), and star fruit (*Averrhoa bilimbi*) from traditional market from Indonesia.

Methods

Preparation of Shrimp Shells Powder and *Averrhoa bilimbi* Extract.

The shrimp shells are washed with clean water and then dried in the sun. After being dried, the shrimp shells are crushed using a blender to obtain shrimp shell powder. *Averrhoa bilimbi* fruit is first cleaned and washed with running water, then extracted using a juicer. The volume of *Averrhoa bilimbi* extract is measured for use in the demineralization process.

Response Surface Methodology (RSM)

This research used the Response Surface Methodology (RSM) with a Central Composite Design (CCD) (Das and Bal, 2025). The research design was developed using Design Expert 10.01 (DX 10.01) software to determine the optimal treatment for the demineralization process. The design used has two independent variables citric acid concentration, and soaking time. The ash content is determined as the optimized response variable, also known as the dependent variable (Y). Table 1 shows the determination of the range and level of the independent variable.

Table 1. Determination of independent variables and treatment

Independent Variable	Range & Level		
	-1	0	+1
Citric acid concentration (%)	10	20	30
Soaking time (minutes)	60	90	120

The experimental data were analyzed using Design Expert software version 10.0.1 (Stat-Ease Inc., USA) with Response Surface Methodology (RSM) and Central Composite Design (CCD). ANOVA and quadratic model selected based on model summary statistics and goodness-of-fit criteria in Design-Expert, were used to evaluate the effects of extraction variables and

determine the optimum demineralization conditions for eco-friendly chitosan extraction. Furthermore, the optimization criteria and expected response will be determined as shown in Table 2.

Table 2. The setting criteria of optimization

Factor and Response	Criteria
Citric acid Concentration (%)	In range
Soaking time (minutes)	In range
Ash content (%)	minimize

The optimization constraints that have been set will produce an optimum condition. The optimum treatment selection will be based on the highest desirability value (Das and Bal, 2025). After obtaining the optimum points, the process continues the verification process based on the predictions set by the program. The verification process is an action to prove that a particular method produces optimum results. The results of program predictions and verification based on laboratory experiments are compared with calculations in Design Expert 10.01, using the paired t-test. The expected result is a p-value>0.05 (not significantly different). After the verification process is carried out for the optimum results, proceed to the next stage, which is characterization.

Chitosan Extraction

The production of chitosan from shrimp shells was carried out based on research methods (Pravitri et al., 2025). Chitosan production was initiated with the preparation of raw materials, including the production of shrimp shell powder and Averrhoa bilimbi extract. Shrimp shell powder was prepared by washing the shrimp shells under running water, followed by sun-drying until a constant dry condition was achieved. The dried shells were then ground using a blender to obtain shrimp shell powder. Meanwhile, Averrhoa bilimbi extract was prepared by first cleaning and washing fresh Averrhoa bilimbi fruits under running water, followed by juice extraction using a juicer. The extracted juice was measured volumetrically and subsequently used in the demineralization process. The process of extracting chitosan from shrimp shells consists of deproteinization, demineralization, and deacetylation. The deproteinization process begins by soaking shrimp shell powder in a 3% NaOH solution (1:10 (g/mL)) at 100°C for 2 hours, then rinsing until the pH is neutral using distilled water. The mixture is then filtered and dried using a cabinet dryer. Subsequently, a demineralization process was carried out using a combination of *Averrhoa bilimbi* extract and citric acid solution. The *Averrhoa bilimbi* extract volume was determined by subtracting the citric acid solution volume (as per the concentration established by Design-Expert) from the total desired solution volume, ensuring the combined acid solution reached 100% of the total volume.

Shrimp shells were initially demineralized by immersion in an acid solution at a ratio of 1:5 (g/mL) and a temperature of 70°C. The duration of this immersion was precisely determined by Design-Expert software. Following demineralization, the shells were rinsed with distilled water until a neutral pH was achieved, then filtered and dried in a cabinet dryer. The subsequent deacetylation process involved soaking the resulting chitin in a 20% NaOH solution at a ratio of 1:10 (g/mL) at 80°C for 2 hours. The chitosan was then filtered, washed with distilled water until neutral pH, and dried to a constant weight, yielding Vannamei shrimp shell chitosan. The obtained chitosan was weighed to determine its percentage yield, and its ash content was subsequently analyzed.

Characterization of Chitosan

The yield value of chitosan is calculated based on the ratio between the weight of chitosan obtained and the weight of shrimp shells at the beginning of the process (Osiriphun et al., 2025). Proximate analysis of chitosan was performed to determine the content of moisture, ash, protein, and fat, which were analyzed according to the standard procedures established by the Association of Official Analytical Chemists (AOAC, 2023). Otherwise, total carbohydrate was calculated by difference, protein, fat, moisture, and ash (g/100 g food) (Smanalieva et al., 2025). The physical and structural characteristics of chitosan were evaluated through color analysis, which was performed using a color reader, the CIE Lab* scale (Hussein et al., 2021).

Scanning Electron Microscopy (SEM) (JEOL 6400, Japan) to analyze the elemental composition of the chitosan samples, and to visualize the morphology of the chitosan samples (Tertsegha et al., 2024). X-ray Fluorescence techniques were carried out on chitosan extracted to determine its mineral composition (Seangarun et al., 2025).

Results and Discussion

Effect of citric acid concentration and soaking time on the Ash content response in chitosan

The fit summary results show that the quadratic model is the most appropriate model to explain the relationship between citric acid concentration (X_1) and immersion time (X_2) on ash content (Table 2). Table 3 showed the sequential model sum of squares, the Quadratic vs 2FI model had a significant effect on the response ($p<0.0001$), while the lack of fit test showed insignificant results ($p=0.0913$). Thus, the quadratic model is recommended as the best model and can adequately represent the experimental data. Meanwhile, the cubic model cannot be considered because it is aliased. (Iancu et al., 2016) state that at 5% level of significance, a model is considered significant if the p-value is less than 0.05, and as stated by Harish et al., (2023) quadratic model was found to be the best fit for retention time and peak area, as their p-values were found to be less than 0.0001. These findings are in line with the underlying statistical principle, which emphasizes that the adequacy of a model is strongly supported by the insignificance of the lack of fit test, as further elaborated by Hosney et al., (2025). The model summary statistics further confirm the suitability of the quadratic model, with values of $R^2 = 0.9846$, Adjusted $R^2 = 0.9736$, and Predicted $R^2 = 0.9100$. The high R^2 values obtained in this study are consistent with findings frequently reported by Borode & Olubambi, (2023), who demonstrated that the quadratic model achieved an Adjusted R^2 of 0.984 and a Predicted R^2 of 0.9721, confirming its superior predictive accuracy. In addition, the low PRESS value (0.41) and Adeq Precision of 29.137 (>4) indicate that the model has sufficient

accuracy and signal to be used in optimization. Similar findings were reported by Sajedifar et al., (2024), who demonstrated that a lower PRESS value compared to the linear model significantly improved prediction accuracy. These consistent observations confirm that the quadratic model employed in this study provides robust validation and reliable predictive power for the response variable. In addition, a ratio greater than 4 is desirable, and hence the ratio of 13.069 implies an adequate signal (Rajewski and Dobrzyńska-Inger, 2021).

Based on these results, the quadratic model can be considered significant and suitable for predicting ash content responses based on variations in citric acid concentration and immersion time. This model provides a solid basis for understanding variable interactions and enables a more accurate determination of optimal process conditions.

ANOVA for Response Surface Quadratic model

The ash content of chitosan extracted ranged from 7.48% to 48.85%. The quadratic model obtained from Response Surface Methodology (RSM) analysis shows that the relationship equation between the independent variables of citric acid concentration (X_1) and immersion time (X_2) and the response of ash content is in the form of a natural logarithm transformation, as described in Equation (1). Data transformations are applied to stabilize the variance and/or to achieve normality. Natural log transformation was used in this study, resulting in data variance with a quadratic function of the mean. According to Nshizirungu et al., (2024) Log transformation and square root transformation are frequently used.

$$\text{Ln (Ash Content)} = 7.41936-0.29779X_1-0.031440X_2+3.77083\times10^{-4}X_1X_2+5.38717\times10^{-3}X_1^2+8.33022\times10^{-5}X_2^2 \quad (1)$$

The results of the analysis of variance (ANOVA) show that this quadratic model is statistically significant with an F value of F = 89.36 and a p value <0.0001, indicating that this model is highly significant and was able to explain the data variation (Wardhani et al., 2024). The R^2 value = 0.9846 and Adjusted R^2 = 0.9736 indicate that the model described more than 97% of the response diversity, while the Predicted R^2 value = 0.9100 was within the range appropriate for Adjusted R^2 (difference < 0.2). The closer the R-Square value is to 1, the better the model adequacy (Peng et al., 2020). The Adeq Precision value = 29.137 (>4) also indicates that the model signal was strong enough to be used in determining the optimum conditions. In addition, RSM has become broadly employed in the food industry sectors for optimization of extraction processes [40].

Individually, the factors of citric acid concentration (X_1), soaking time (X_2), and the quadratic effect of citric acid concentration (X_1^2) had a significant effect on ash content ($p < 0.05$). In contrast, the interaction between X_1 and X_2 ($p = 0.0591$) and the quadratic effect of immersion time (X_2^2) ($p = 0.0898$) were not significant at the 95% confidence level, but were retained in the model to maintain the hierarchy of the equation. The Lack of Fit value F = 4.46 with p = 0.0913 indicates that the lack of fit is not significant; therefore, the model fits the experimental data.

According to the equation obtained, the model shows that an increase in citric acid concentration (X_1) tends to decrease ash content linearly (negative coefficient), but at higher levels, the quadratic effect (X_1^2) becomes significant and actually increases ash content. This indicates an optimum point in the use of citric acid concentration. The decrease in ash content with increasing citric acid addition can be attributed to the ability of citric acid to chemically interact with inorganic mineral constituents of the biomass, thereby promoting their dissolution and subsequent removal. Through complexation with metal ions, citric acid facilitates the formation of soluble complexes that are readily eliminated during washing, ultimately resulting in a substantial decrease in the overall ash content (Syandri et al., 2025). However, Tissera et al., (2021) confirmed this research and found that a 25% citric acid concentration provided the best demineralization.

Meanwhile, the soaking time (X_2) also reduces the ash content linearly, although its quadratic effect is relatively weak. These results are in line with research conducted by Głąb et al., (2021), which reported that longer immersion allows for a more complete diffusion of soluble minerals out of the material matrix. Demineralization efficiency increases with longer immersion times until equilibrium is reached. However, once diffusion has reached equilibrium, extending the immersion time does not result in significant improvement.

Based on the results of the ANOVA analysis, this RSM Quadratic model can be used to predict the ash content based on variations in citric acid concentration and soaking time, as well as to determine the optimal combination of conditions in the soaking process. Figure 1 shows the contour plot surface, and Figure 2 shows the 3D response surface plot of the optimization results with total ash content response.

Verification

The results then proceed to the optimization stage, in which Design Expert 10.01 predicts the optimum conditions based on the experimental data. According to the optimization results, the predicted optimal point for the demineralization of shrimp shells in the chitosan extraction process was obtained at a citric acid concentration of 25.260 and an immersion time of 100.470, with a desirability value of 1.000. According to Luis Pérez, (2021), the desirability value ranges from 0 to 1. The higher the desirability value, the more desirable the factors are in terms of giving the desired response, and correspond to the optimal performance for the studied factors. According to (Hejazi, 2022), A desirability value exceeding 0.8 is regarded as an

acceptable threshold for implementing a specific objective function, while values approaching 1 indicate superior optimization efficiency. Thus, under these conditions, the process is expected to achieve the most favorable outcome for shrimp shell demineralization in chitosan extraction.

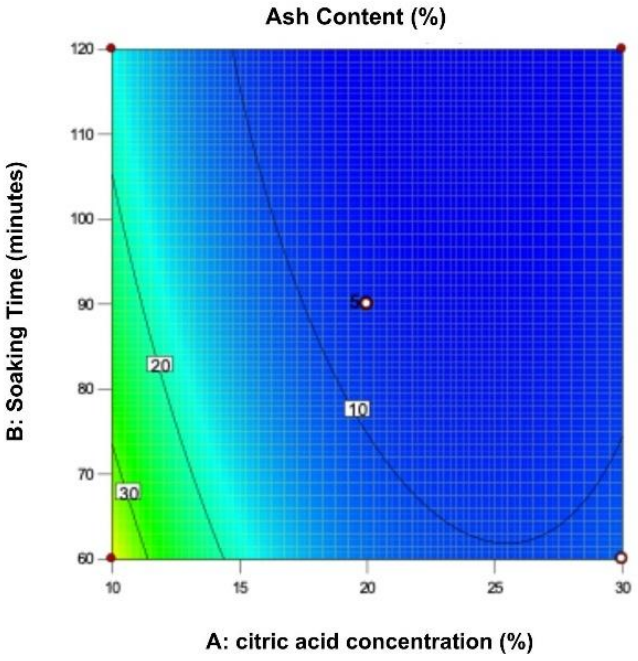

Figure 1. Contour Plot Surface

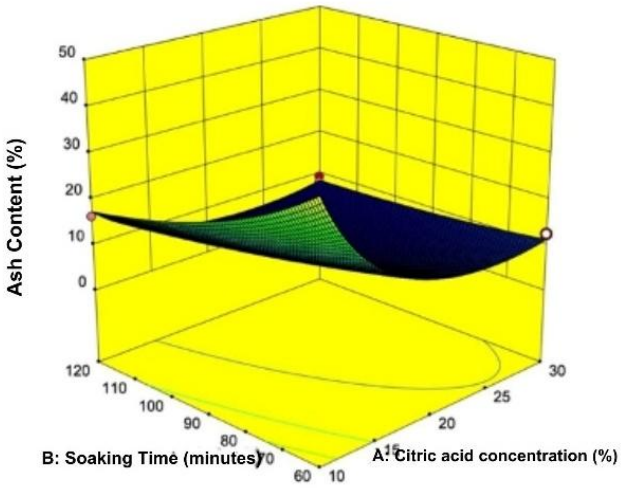

Figure 2. 3D Response Surface Plot

The optimization point predicted by this design expert is in line with research conducted by (Tissera et al., 2021), which states that a 25% (w/v) citric acid concentration provides the best demineralization by removing almost all mineral components present in the pretreated shells. Meanwhile, the optimum soaking time predicted by the Design Expert 10.01 in this study is in accordance with what is stated by Younes & Rinaudo, (2015). The demineralization process using HCl is carried out for 2-3 hours with stirring, but the reaction time varies depending on the preparation method, so it can take anywhere from 15 minutes to several hours. This study shows that the optimal concentration is within a certain range, not at the highest concentration and time.

Table 4. Comparison of Prediction and Verification Results

	Ash content (%)
Prediction	7.236 ± 0.028
Verification	7.464±0.234
P-Value	0.793

The process optimization results obtained were then verified by conducting three replications of the experiment. Based on the verification results (Table 4), the ash content of the experimental results was consistent with the predicted values generated by Design Expert 10.01. The statistical paired t-test analysis showed that the ash content between the predicted and experimental values had a $p > 0.05$, indicating no significant difference. Therefore, it can be stated that the prediction model and the experimental verification were in close agreement, confirming the validity and reliability of the optimization results for the demineralization process of shrimp shells in chitosan extraction.

Characterization of the optimized chitosan

Table 5 shows the comparison between the physicochemical characteristics of optimized chitosan produced through citric acid demineralization and commercial chitosan. The optimized chitosan yielded 11.36%, which is within the range reported by previous studies using HCl (15.80%) and H_2SO_4 (17.22%). However, it is lower than the extraction results using organic acids such as citric acid, acetic acid, and lactic acid as demineralizing agents, with yields of 25.33%, 23.56%, and 24.47%, respectively (El-Araby et al., 2022).

Ash content of the optimized chitosan (7.46%) was slightly lower than that of commercial chitosan (7.81%), suggesting that the demineralization process effectively reduced the mineral fraction. However, this result is higher than the findings conducted by El-Araby et al. (2022), which produced chitosan with an ash content ranging from 0.02 to 0.5. This may be due to the demineralization process, which takes up to 24 hours, and constant stirring, resulting in longer contact between the material and the solvent. However, this process has disadvantages because it is not sufficiently efficient and requires a large amount of energy (Hosney et al., 2022; Vicente et al., 2024). Based on the results of analysis using X-ray Fluorescence, the minerals contained in the optimized and commercial chitosan are aluminum (Al), silicon (Si), phosphorus (P), sulfur (S), titanium (Ti), chromium (Cr), manganese (Mn), Iron (Fe), Nickel (Ni), Copper (Cu), Zinc (Zn), Silver (Ag), and Tin (Sn). Meanwhile, calcium ions in calcium carbonate (CaCO3), which are the main component of shrimp shells in protein-chitin-calcium carbonate bonds, were not detected in commercial chitosan but were still detected in optimized chitosan at 4.37%. Then, several mineral ions such as strontium (Sr), cadmium (Cd), tantalum (Ta), and barium (Ba) were also still detected at 0.0326%; 0.0008%; 0.0014%, respectively.

Table 5. Comparison of the characteristics of optimized and commercial chitosan

Parameter	Chitosan	
	Optimized	Commercial
Yield (%)	11.36±0.004	-
Ash (%)	7.46±0.23	7.81±0.59
Water (%)	11.52±0.52	8.58±0.16
Protein (%)	0.49±0.24	31.63±1.29
Lipid (%)	0.06±0.01	0.06±0.01
Carbohydrate (%)	80.45±1.22	51.93±0.55
Color		
L*	75.84±0.35	91.30±0.15
a*	7.55±0.222	6.30±0.13
b*	22.52±0.26	3.57±0.09
Degree of Deacetylation (DD)	65.98%	76.42%

Water content in the optimized chitosan was higher (11.52%) compared to the commercial sample (8.58%), These results are within the range of moisture content obtained (Mahin et al., 2025), which yielded 8.68% chitosan from the extraction. However, according to (Hosney et al., 2025), commercial chitosan contains around 0,26% moisture content. Nevertheless, these results are in line with which states that the water content of chitosan is in the range of 0,26-0,51% (Hosney et al., 2025). This shows that the optimized chitosan retained more water than the commercial chitosan. Variations in the water content of the biopolymers produced are probably influenced by differences in the ability of chitin and chitosan biopolymers to absorb water after undergoing several stages of synthesis, so that differences in the synthesis process and source of chitosan will affect the water content of the chitosan produced (Olaosebikan et al., 2021).

In terms of proximate other composition, the optimized chitosan contained significantly lower protein (0.49%) than commercial chitosan (31.63%). The optimization results in this study showed a much lower protein content compared to the protein content of commercial chitosan, confirming the efficiency of the deproteinization step. Based on the results obtained Olaosebikan et al., (2021), Chitosan extracted from shrimp shell waste has a protein content of between 3.65-3.80%, which is not too far off from the results of this study. Meanwhile, Mahin et al., (2025) found chitosan protein content was closer when compared to the chitosan in this study.

Lipid content was very low and comparable between samples (0.06%), in agreement with prior findings by Olaosebikan et al., (2021). The extracted lipids showed slightly higher results, approximately 2.00 to 2.60%. Meanwhile, the chitosan used in the study by Mahin et al., (2025) showed very low lipid content analysis results, which were undetectable using the analysis method performed. Interestingly, the carbohydrate fraction of optimized chitosan was substantially higher (80.45%) than that of commercial chitosan (51.93%). The results of this study show a carbohydrate content nearly Similar to the research conducted by (Olaosebikan et al., 2021), which shows that chitosan extracted from shrimp shell waste has a carbohydrate content of 77.55% to 79.18%. Reflecting the higher purity of polysaccharide chains obtained from the optimized chitosan extraction process.

Color analysis revealed noticeable differences between the samples. Optimized chitosan exhibited lower lightness (L* = 75.84) compared to commercial chitosan (L* = 91.30), indicating a slightly darker appearance. Meanwhile, the a* and b* values of optimized chitosan (7.55 and 22.52, respectively) were higher than those of commercial chitosan (6.30 and 3.57), suggesting a more reddish and yellowish hue. This color difference may be due to the use of different acid sources in the chitosan extraction process, where optimized chitosan uses a mixture of citric acid and *Averrhoa bilimbi* extract, which contains natural pigments and phenolic compounds that can affect the color of the resulting chitosan. *Averrhoa bilimbi* is known to contain flavonoid pigments that contribute to its yellowish color (Fajriani et al., 2024). According to another study, the interaction between citric acid and phenolic compounds contained in *Averrhoa bilimbi* extract produces a brownish color. Iwansyah et al., (2021) found that citric acid solution is one of the best solvents compared to other organic acids for the extraction of phenolic compounds, so the presence of citric acid can increase the extraction and stability of phenolic compounds that contribute to a darker color in the resulting chitosan. Meanwhile, commercial chitosan usually uses pure acids such as hydrochloric acid and acetic acid. In addition, the commercial chitosan typically undergoes extensive purification and bleaching processes that remove natural pigments and organic impurities. Therefore, the altered extraction conditions can affect the final product's appearance (El-Araby et al., 2022).

Degree of deacetylation (DD) is one of the main parameters determining the quality, purity, and functional properties of chitosan. Higher DD values indicate greater removal of acetyl groups from chitin, resulting in chitosan with higher reactivity, improved solubility in acidic solutions, and broader potential for biomedical, pharmaceutical, and food applications (Ghanem et al., 2025). The optimized chitosan exhibited a DD value of 65.98%, which is classified as a moderate degree of deacetylation. Chitosan with DD values ranging from 50–70% is generally considered suitable for various applications, although its reactivity, solubility, and film-

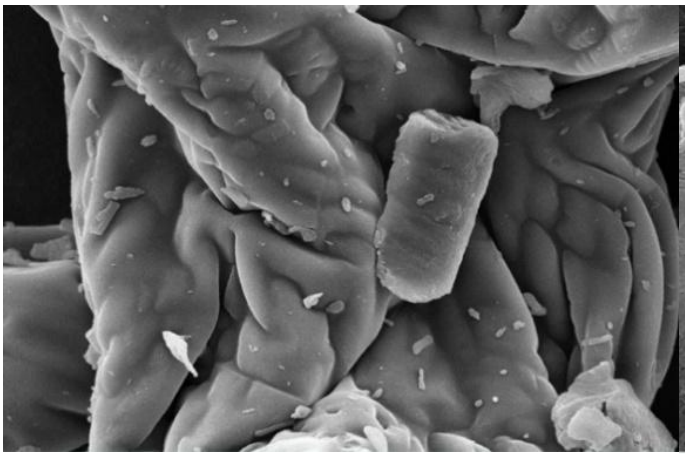

Figure 3. Optimized Chitosan Morphology (2000x)

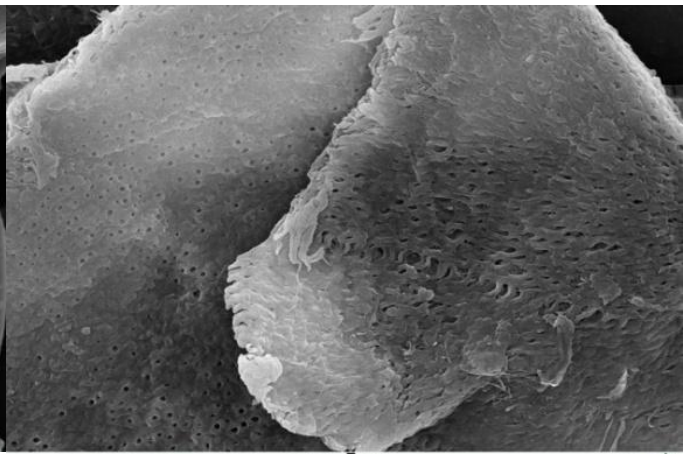

Figure 4. Commercial Chitosan Morphology (2000x)

forming properties may be lower than those of highly deacetylated chitosan (Kadak et al., 2023; Ghanem et al., 2025).

In contrast, the commercial chitosan showed a DD value of 76.42%, which falls within the high DD category (approximately 70–95%). Chitosan with higher DD values is generally preferred for food, pharmaceutical, and biomedical applications due to its improved physicochemical properties and higher biocompatibility. The higher degree of deacetylation is associated with more extensive removal of acetyl functional groups during the deacetylation process (Kadak et al., 2023; Sánchez-Machado et al., 2024; Ghanem et al., 2025) . In addition, DD is closely related to chitosan purity, where higher DD values indicate higher chitosan purity levels (Widyastuti, 2023; Ghanem et al., 2025; Sarofa et al., 2025).

Based on the comparative analysis, the optimized chitosan demonstrated competitive quality relative to commercial chitosan, particularly in terms of lower protein residue, lower ash content, and higher carbohydrate purity. However, differences were observed in color characteristics and degree of deacetylation (DD), where the optimized chitosan exhibited a moderate DD value compared to the higher DD of commercial chitosan. Despite this difference, the optimized chitosan still showed physicochemical characteristics suitable for potential food biopolymer applications. These findings confirm that citric acid-based demineralization combined with *Averrhoa bilimbi* extract can produce chitosan with desirable properties while supporting environmentally friendly and sustainable extraction approaches as alternatives to conventional mineral acid-based methods.

Chitosan Morphological

The morphological characteristics of optimized chitosan and commercial chitosan were analyzed using Scanning Electron Microscopy (SEM). The SEM micrographs of optimized chitosan (Figure 3) showed a heterogeneous and porous surface structure with interconnected cavities of varying sizes, indicating effective mineral removal during the extraction process. The porous morphology may support water interaction and film-forming properties important for biodegradable food packaging and edible coating applications. Similar porous structures in chitosan extracted using organic acid treatments were also reported by El-Araby et al. (2022), who observed fibrous and porous surface characteristics associated with organic acid extraction processes.

In contrast, the commercial chitosan sample (Figure 4) exhibited a more compact and homogeneous morphology with smoother layered surfaces and lower porosity. Similar structural characteristics were reported by Ghanem et al., (2025), who described commercial chitosan as having dense and relatively uniform surface structures compared to laboratory-extracted chitosan samples.

FTIR Analysis of Chitosan Functional Groups

FTIR analysis was conducted to identify the functional group characteristics of the optimized chitosan compared to commercial chitosan as a reference material. The FTIR spectra presented in Figure 5 showed that the optimized chitosan exhibited spectral patterns generally similar and consistent with the characteristic structure of commercial chitosan. However, several shifts in wavenumber were observed, indicating possible differences in purity level, hydrogen bond interactions, and degree of deacetylation between the samples.

Table 6 shows that the FTIR spectral patterns of optimized chitosan and commercial chitosan were generally similar, although several shifts in wavenumber indicated relevant differences in their chemical structures. The –OH absorption bands observed at 3452.23 cm^{-1} (optimized chitosan) and 3401.15 cm^{-1} (commercial chitosan), which fall within the characteristic range of hydroxyl groups (3200–3570 cm^{-1}) and dimeric OH groups (3450–3550 cm^{-1}), indicated the presence of strong hydrogen bonding interactions in both samples. The slightly higher peak position in optimized chitosan suggested a potentially more ordered hydrogen bonding arrangement. Previous studies reported amide N–H absorption bands at 3369.11–3413.07 cm^{-1} in commercial chitosan (Sarbon et al., 2015), while another study identified absorption bands at 3443 cm^{-1} corresponding to O–H and N–H stretching vibrations (Ahing and Wid, 2016).

The asymmetric and symmetric C–H stretching vibrations detected at 2932 cm^{-1} (optimized chitosan) and 2927 cm^{-1} (commercial chitosan) were within the typical methylene stretching range (2915–2935 cm^{-1}), indicating the integrity of methylene groups in both

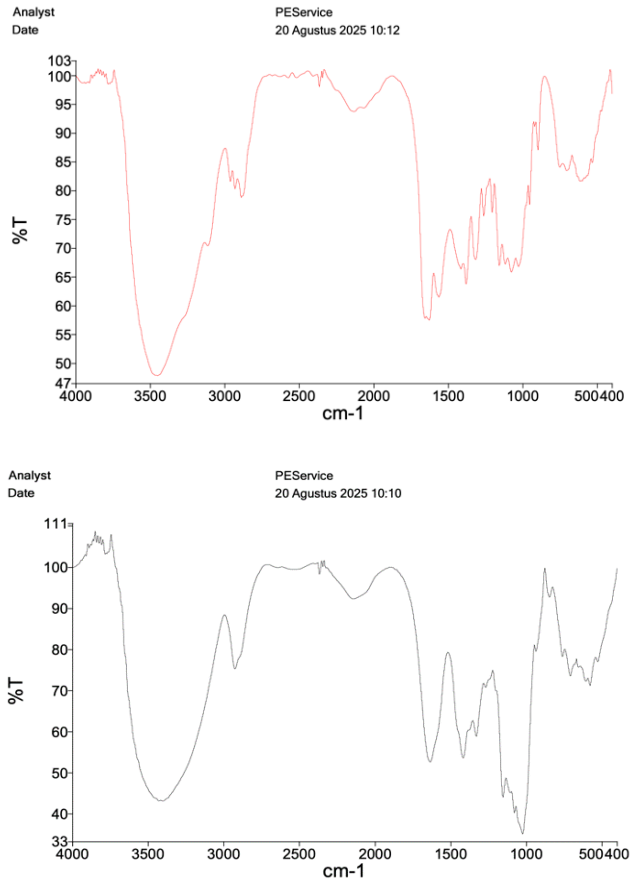

Figure 5. FTIR Spectra of (a) Optimized Chitosan and (b) Commercial Chitosan

Table 6. Comparison of Functional Group Characterization between Optimized and Commercial Chitosan

No	Functional Group	Wavenumber (cm^{-1})		Functional Group Assignment	Wavenumber Range (cm^{-1})	Reference
		Optimized	Commercial			
1	OH stretch, H-OH stretch, OH and N-H Streching	3452.23	3401.15	• Alcohol and hydroxyl compounds (hydroxyl group/dimeric OH) • Amine group	• 3200-3570 • 3450-3550 • 3420-3443	(Ahing and Wid, 2016; Nandiyanto et al., 2023; Elhaes et al., 2024)
2	C-H Asym/sym strech	2932.84	2927.65	• Methylene group	• 2915–2935	(Nandiyanto et al., 2023)
3	C=O strech	1627.92	1635.17	• Olefinic compounds (alkene/alkenyl)	• 1620-1680	(Elhaes et al., 2024)
4	C-H in-plane bend	1414.99	1416.87	• Olefinic compounds (vinyl alkene)	• 1410-1420	(Nandiyanto et al., 2023)
5	C–O stretch	1156.98	1154.36	• Alcohol and hydroxyl compounds (tertiary alcohol)	• 1150-1160	(Nandiyanto et al., 2023)
6	C-O stretch	1076.38	1078.51	• Ether and oxy compounds (alkyl-substituted ether)	• 1050-1150	(Nandiyanto et al., 2023)
7	C-Cl stretch	703.75	708.17	• Aliphatic organohalogen compounds (aliphatic chloro compounds)	• 700-800	(Nandiyanto et al., 2023)

samples. In addition, the C=O stretching bands observed at 1627.92 cm^{-1} (optimized chitosan) and 1635.17 cm^{-1} (commercial chitosan) corresponded to olefinic functional groups, particularly alkenyl structures within the range of 1620–1680 cm^{-1}. The in-plane C–H bending vibrations detected at 1414 cm^{-1} (optimized chitosan) and 1416 cm^{-1} (commercial chitosan) indicated vinyl alkene groups, while the C–O vibrational bands at 1156–1154 cm^{-1} and 1076–1078 cm^{-1} confirmed the polysaccharide backbone structure and deacetylation characteristics of chitosan, corresponding to tertiary alcohol (1150–1160 cm^{-1}) and alkyl ether functional groups (1050–1150 cm^{-1}). At lower wavenumbers (703 and 708 cm^{-1}), the presence of C–Cl vibrations within the range of 700–800 cm^{-1} suggested trace amounts of organohalogen compounds, particularly aliphatic chloro compounds (Nandiyanto et al., 2023; Elhaes et al., 2024).

Based on these results, the distribution of absorption bands indicated that the optimized chitosan possessed a more ordered chemical structure with stronger hydrogen bonding interactions. Stronger and more organized intermolecular and intramolecular hydrogen bonding networks may cause absorption peaks to shift toward higher wavenumbers, as observed in the optimized chitosan sample (Pramitha et al., 2021; Kızılkaya and Kaya, 2024). Intermolecular hydrogen bonds occur between different molecules, whereas intramolecular hydrogen bonds occur within the same molecule. During chitosan formation, random glycosidic bond cleavage and deacetylation reactions may occur, resulting in structural heterogeneity and variations in polymer chain length. Such structural heterogeneity can reduce the strength of intermolecular and intramolecular hydrogen bonding within the chitosan matrix. However, when the deacetylation process is not fully optimized, stronger hydrogen bonding interactions may still be retained, leading to a more compact and ordered polymer chain arrangement (Purnawan et al., 2012). These strong hydrogen bonding interactions may also reduce water penetration, thereby affecting the solubility properties of chitosan.

Conclusion

This study successfully optimized the eco-friendly extraction of chitosan from Vannamei shrimp shell waste using a combination of citric acid and *Averrhoa bilimbi* extract through Response Surface Methodology (RSM). The optimum condition was achieved at 25.260% citric acid concentration and 100.470 minutes soaking time, producing chitosan with lower ash and protein contents, higher carbohydrate purity, and a porous morphology compared to commercial chitosan. These findings indicate that natural organic acids have potential as environmentally friendly alternatives to mineral acids for sustainable chitosan production and food biopolymer applications.

Acknowledgments

We would like to express our gratitude to Direktorat Penelitian dan Pengabdian kepada Masyarakat, Kementerian Pendidikan Tinggi, Sains, dan Teknologi for providing funding support through the Penelitian Dosen Pemula 2025.

References

Affes, S., Aranaz, I., Acosta, N., Heras, Á., Nasri, M., Maalej, H. 2024. Physicochemical and biological properties of chitosan derivatives with varying molecular weight produced by chemical depolymerization. Biomass Conversion and Biorefinery 14(3):. DOI:10.1007/s13399-022-02662-3.

Ahing, F.A., Wid, N. 2016. Optimization of shrimp shell waste deacetylation for chitosan production. International Journal of Advanced and Applied Sciences 3(10):. DOI:10.21833/ijaas.2016.10.006.

AOAC. 2023, January 4. Official Methods of Analysis of AOAC INTERNATIONAL. Latimer Jr., G. W. (Ed). Oxford University Press. DOI:10.1093/9780197610145.001.0001.

Artilia, I., Dewi, Z.Y., Shofiani, W., Auli, W.N., Ahmad, N. 2023. Extraction and Characterization of Chitosan from Eco-Green *Hermetia Illucens* for Application in Dentistry. Key Engineering Materials 965. DOI:10.4028/p-p8henm.

Borode, A., Olubambi, P. 2023. Modelling the effects of mixing ratio and temperature on the thermal conductivity of GNP-Alumina hybrid nanofluids: A comparison of ANN, RSM, and linear regression methods. Heliyon 9(8):. DOI:10.1016/j.heliyon.2023.e19228.

Das, P., Bal, M. 2025. Modeling and optimization study for microplastic removal from aquatic medium using Chroococcidiopsis species. Chemical Engineering Science 304. DOI:10.1016/j.ces.2024.121085.

El-Araby, A., Ghadraoui, L. El, Errachidi, F. 2022. Physicochemical properties and functional characteristics of ecologically extracted shrimp chitosans with different organic acids during demineralization step. Molecules 27(23): 8285. DOI: 10.3390/molecules27238285

Elhaes, H., Ezzat, H.A., Ibrahim, A., Samir, M., Refaat, A., Ibrahim, M.A. 2024. Spectroscopic, Hartree–Fock and DFT study of the molecular structure and electronic properties of functionalized chitosan and chitosan-graphene oxide for electronic applications. Optical and Quantum Electronics 56(3):. DOI:10.1007/s11082-023-05978-0.

Espinosa-Solís, A., Velázquez-Segura, A., Lara-Rodríguez, C., Martínez, L.M., Chuck-Hernández, C., Rodríguez-Sifuentes, L. 2024. Optimizing Chitin Extraction and Chitosan Production from House Cricket Flour. Processes 12(3):. DOI:10.3390/pr12030464.

Fajriani, N., Sudarmin, A., Syam, H., Sukainah, A. 2024. Effectiveness of Using Natural Coagulants in Making Koro Pedang Tofu. 2(1): 11–17. DOI: 10.26858/jai.V2i1.63295

Ghanem, S.N., Marzouk, M.I., Tawfik, M.E., Eskander, S.B. 2025. Spectroscopic approaches for structural analysis of extracted chitosan generated from chitin deacetylated for escalated periods. BMC chemistry 19(1): 214. Springer. DOI:10.1186/s13065-025-01558-3.

Głąb, M., Kudłacik-Kramarczyk, S., Drabczyk, A., Guigou, M.D., Sobczak-Kupiec, A., Mierzwiński, D., Gajda, P., Walter, J., Tyliszczak, B. 2021. Multistep

chemical processing of crickets leading to the extraction of chitosan used for synthesis of polymer drug carriers. Materials 14(17):. DOI:10.3390/ma14175070.

Hahn, T., Egger, J., Krake, S., Dyballa, M., Stegbauer, L., Seggern, N. von, Bruheim, I., Zibek, S. 2024. Comprehensive characterization and evaluation of the process chain and products from Euphausia superba exocuticles to chitosan. Journal of Applied Polymer Science 141(2):. DOI:10.1002/app.54789.

Harish, V., Almalki, W.H., Alshehri, A., Alzahrani, A., Gupta, M.M., Alzarea, S.I., Kazmi, I., Gulati, M., Tewari, D., Gupta, G., Dua, K., Singh, S.K. 2023. Quality by Design (QbD) Based Method for Estimation of Xanthohumol in Bulk and Solid Lipid Nanoparticles and Validation. Molecules 28(2):. DOI:10.3390/molecules28020472.

Hazmi, A.D., Taib, A.F.M., Yahya, S., Alias, N.Z. 2024. Oxalic Acid from Averrhoa bilimbi L. as a Bleaching Agent. Malaysian Journal of Chemistry 26(5):. DOI:10.55373/mjchem.v26i5.407.

Hejazi, T.H. 2022. A scenario-based desirability function for correlated multi-response optimization problems considering modeling and implementation errors. Journal of Computational Science 63. DOI:10.1016/j.jocs.2022.101764.

Hilyana, S., Amir, S., Alim, S., Scabra, A.R., Muahiddah, N., Diamahesa, W.A. 2023. Produksi Dan Komersialisasi Udang Vanamei Salinitas Rendah Di Desa Sokong, Lombok Utara. Jurnal Abdi Insani 10(2): 761–770. DOI: 10.29303/abdiinsani.v10i2.950

Hosney, A., Ullah, S., Barčauskaitė, K. 2022. A review of the chemical extraction of chitosan from shrimp wastes and prediction of factors affecting chitosan yield by using an artificial neural network. Marine Drugs 20(11): 675. DOI: 10.3390/md20110675

Hosney, A., Urbonavičius, M., Varnagiris, Š., Ignatjev, I., Ullah, S., Barčauskaitė, K. 2025. Feasibility study on optimizing chitosan extraction and characterization from shrimp biowaste via acidic demineralization. Biomass Conversion and Biorefinery 15(8):. DOI:10.1007/s13399-024-06017-y.

Hussein, E.M., Desoky, W.M., Hanafy, M.F., Guirguis, O.W. 2021. Effect of TiO2 nanoparticles on the structural configurations and thermal, mechanical, and optical properties of chitosan/TiO2 nanoparticle composites. Journal of Physics and Chemistry of Solids 152. DOI:10.1016/j.jpcs.2021.109983.

Iancu, V., Roncea, F., Cazacincu, R.G., Lupu, C.E., Miresan, H., Dănăilă, C.N., Rosca, C., Lupuleasa, D. 2016. Response surface methodology for optimization of diclofenac sodium orodispersible tablets (ODTs). Farmacia 64 210–216.

Iber, B.T., Kasan, N.A., Torsabo, D., Omuwa, J.W. 2022. A review of various sources of chitin and chitosan in nature. Journal of Renewable Materials. DOI:10.32604/jrm.2022.018142.

Iwansyah, A.C., Desnilasari, D., Agustina, W., Pramesti, D., Indriati, A., Mayasti, N.K.I., Andriana, Y., Kormin, F.B. 2021. Evaluation on the physicochemical properties and mineral contents of averrhoa bilimbi l. Leaves dried extract and its antioxidant and antibacterial capacities. Food Science and Technology (Brazil) 41(4):. DOI:10.1590/fst.15420.

Kadak, A.E., Küçükgülmez, A., Çelik, M. 2023. Preparation and characterization of crayfish (Astacus leptodactylus) chitosan with different deacetylation degrees. Iranian Journal of Biotechnology 21(2): e3253. DOI: 10.30498/ijb.2023.323958.3253

Katsoulis, Rovoli. 2021. Optimization of Chitin Extraction, Physicochemical and Functional Properties of Chitosan Production from Shells of Karamote Shrimp Peneaus (Melicertus) Kerathurus in Western Greece. Journal of Veterinary Science & Medicine 9(1):. DOI:10.13188/2325-4645.1000052.

Kızılkaya, P., Kaya, M. 2024. Chitosan/TiO2/Rosmarinic acid bio-nanocomposite coatings: characterization and preparation. Journal of Composites Science 9(1): 2. DOI: 10.3390/jcs9010002

Luis Pérez, C.J. 2021. On the application of a design of experiments along with an anfis and a desirability function to model response variables. Symmetry 13(5):. DOI:10.3390/sym13050897.

Mahin, M.I., Rashid, M.H.-A., Mredul, A.R. 2025. Effects of shrimp chitosan based edible coating on the shelf life of selected vegetables in context of attaining SDGs. Applied Food Research 5(1): 100682. DOI:10.1016/j.afres.2024.100682.

Nandiyanto, A.B.D., Ragadhita, R., Fiandini, M. 2023. Interpretation of Fourier Transform Infrared Spectra (FTIR): A Practical Approach in the Polymer/Plastic Thermal Decomposition. Indonesian Journal of Science and Technology 8(1):. DOI:10.17509/ijost.v8i1.53297.

Nshizirungu, T., Rana, M., Jo, Y.T., Uwiragiye, E., Kim, J., Park, J.H. 2024. Ultrasound-assisted sustainable recycling of valuable metals from spent Li-ion batteries via optimisation using response surface methodology. Journal of Environmental Chemical Engineering 12(2):. DOI:10.1016/j.jece.2024.112371.

Olaosebikan, A.O., Kehinde, O.A., Tolulase, O.A., Victor, E.B. 2021. Extraction and characterization of chitin and chitosan from Callinectes amnicola and Penaeus notialis shell wastes. Journal of Chemical Engineering and Materials Science 12(1):. DOI:10.5897/jcems2020.0353.

Osiriphun, S., Jirarattanarangsri, W., Laokuldilok, T. 2025. Valorization of shrimp waste: Chitosan extraction, formulation, and antimicrobial assessment of a novel antiseptic mouth spray. Food Chemistry Advances 9. DOI:10.1016/j.focha.2025.101178.

Ozel, N., Elibol, M. 2024. Chitin and chitosan from mushroom (Agaricus bisporus) using deep eutectic solvents. International Journal of Biological Macromolecules 262. DOI:10.1016/j.ijbiomac.2024.130110.

Peng, X., Yang, G., Shi, Y., Zhou, Y., Zhang, M., Li, S. 2020. Box–Behnken design based statistical modeling for the extraction and physicochemical properties of pectin from sunflower heads and the

comparison with commercial low-methoxyl pectin. Scientific Reports 10(1):. DOI:10.1038/s41598-020-60339-1.

Pérez, W.A., Marín, J.A., López, J.N., Burgos, M.A., Rios, L.A. 2022. Development of a Pilot-ecofriendly Process for Chitosan Production from Waste Shrimp Shells. Environmental Processes 9(3):. DOI:10.1007/s40710-022-00605-8.

Pramitha, V.S., Sajeetha, S.B., Alsif, H., Aiswarya, A., Fathima, J.A.R., Aryaraj, D. 2021. Characterization and bioactivity study of chitosan based nanomaterial from exoskeleton waste of Parapaeneopsis stylifera. Research Square. DOI: 10.21203/rs.3.rs-508681/v1

Pravitri, K.G., Naufali, M.N., Hidayatullah, A. 2025. Testing the effectiveness of vannamei shrimp shell chitosan extraction with variations of organic acids in the demineralization stage: Pengujian Efektivitas Ekstraksi Kitosan Kulit Udang Vannamei dengan Variasi Jenis Asam Organik dalam Tahapan Demineralis. JITIPARI (Jurnal Ilmiah Teknologi dan Industri Pangan UNISRI) 10(1): 78–90. DOI: 10.33061/jitipari.v10i1.11536

Psarianos, M., Ojha, S., Schneider, R., Schlüter, O.K. 2022. Chitin Isolation and Chitosan Production from House Crickets (Acheta domesticus) by Environmentally Friendly Methods. Molecules 27(15):. DOI:10.3390/molecules27155005.

Purnawan, C.P.C., Wibowo, A.H.W.A.H., Samiyatun, S. 2012. Kajian Ikatan Hidrogen Dan Kristalinitas Kitosan Dalam Proses Adsorbsi Ion Logam Perak (Ag). Molekul 7(2): 121–129.

Rajewski, J., Dobrzyńska-Inger, A. 2021. Application of response surface methodology (Rsm) for the optimization of chromium(iii) synergistic extraction by supported liquid membrane. Membranes 11(11):. DOI:10.3390/membranes11110854.

Sajedifar, J., Mortazavi, S.B., Mahabadi, H.A. 2024. Performance analysis, statistical modeling, and multiple response optimization of a novel fixed-bed quartz reactor packed with Ba-Pt@ γ-AL2O3 using response surface methodology. Heliyon 10(19): e38087. Elsevier. DOI:10.1016/j.heliyon.2024.e38087.

Sánchez-Machado, D.I., López-Cervantes, J., Escárcega-Galaz, A.A., Campas-Baypoli, O.N., Martínez-Ibarra, D.M., Rascón-León, S. 2024. Measurement of the degree of deacetylation in chitosan films by FTIR, 1H NMR and UV spectrophotometry. MethodsX 12. DOI:10.1016/j.mex.2024.102583.

Sarbon, N.M., Sandanamsamy, S., Kamaruzaman, S.F.S., Ahmad, F. 2015. Chitosan extracted from mud crab (Scylla olivicea) shells: physicochemical and antioxidant properties. Journal of food science and technology 52(7): 4266–4275. DOI: 10.1007/s13197-014-1522-4

Sarofa, U., Rosida, D.F., Khafsa, N. 2025. The role of base types and concentration in the deacetylation process of manufacturing chitosan from green mussel shells (Perna viridis). Food Research 9(1):. DOI:10.26656/fr.2017.9(1).405.

Seangarun, C., Seesanong, S., Boonchom, B., Laohavisuti, N., Rungrojchaipon, P., Boonmee, W., Punthipayanon, S., Thongkam, M. 2025. Extraction of Chitin, Chitosan, and Calcium Acetate from Mussel Shells for Sustainable Waste Management. International Journal of Molecular Sciences 26(15):. DOI:10.3390/ijms26157107.

Septiani, I., Supriyo, E. 2022. Optimasi Pembuatan Kitosan Dari Limbah Cangkang Bekicot (Achatina fulica) Menggunakan Factorial Design 2 Pangkat 3. METANA 18(1): 65–70. Universitas Diponegoro. DOI: 10.14710/metana.v18i1.46292

Sheikh, M., Mehnaz, S., Sadiq, M.B. 2021. Prevalence of fungi in fresh tomatoes and their control by chitosan and sweet orange (Citrus sinensis) peel essential oil coating. Journal of the Science of Food and Agriculture 101(15):. DOI:10.1002/jsfa.11291.

Smanalieva, J., Iskakova, J., Musulmanova, M., Giertlová, A., Porubská, J. 2025. Development of Kyrgyz food composition tables: Limitations and challenges. Journal of Food Composition and Analysis 143. DOI:10.1016/j.jfca.2025.107567.

Syandri, H., Azrita, A., Elfrida, E., Aryani, N. 2025. Functional characterization of gelatin from freshwater fish scales using Averrhoa bilimbi acid pretreatment. AACL Bioflux 18(2):.

Tertsegha, S., Akubor, P.I., Iordekighir, A.A., Christopher, K., Okike, O.O. 2024. Extraction and characterization of chitosan from snail shells (Achatina fulica). Journal of food quality and hazards control 11(3): 186–196. DOI: 10.18502/jfqhc.11.3.16590

Tissera, W.M.J.C.M., Rathnayake, S.I., Abeyrathne, E.D.N.S., Nam, K.-C. 2021. An improved extraction and purification method for obtaining high-quality chitin and chitosan from blue swimmer (Portunus pelagicus) crab shell waste. Food science and biotechnology 30(13): 1645–1655. Korea (South). DOI:10.1007/s10068-021-01002-x.

Tkachenko, I. V., Antonenko, A.M., Vavrinevych, O.P., Omelchuk, S.T., Bardov, V.G. 2022. Substantion Of The Need For Monitoring In Environmental Objects Of Insecticides From The Class Of Tetramic And Tetronic Acid Derivatives Taking Into Account Their Specific Influence On The Human Organism. Wiadomosci lekarskie (Warsaw, Poland : 1960) 75(6):. DOI:10.36740/wlek202207109.

Vicente, F.A., Hren, R., Novak, U., Čuček, L., Likozar, B., Vujanović, A. 2024. Energy demand distribution and environmental impact assessment of chitosan production from shrimp shells. Renewable and Sustainable Energy Reviews 192. DOI:10.1016/j.rser.2023.114204.

Wang, J., Zhuang, S. 2022. Chitosan-based materials: Preparation, modification and application. Journal of Cleaner Production 355 131825. DOI: 10.1016/j.jclepro.2022.131825

Wardhani, L.A.K., Arifilla, T.D., Karaman, N. 2024. Pembuatan Tembaga Sulfat dari Limbah Padat Tembaga dengan Proses Kristalisasi Panas. G-Tech: Jurnal Teknologi Terapan 8(3): 1931–1939. DOI:10.33379/gtech.v8i3.4680.

Widyastuti, W. 2023. Perbandingan Karakteristik Dan Kualitas Kitosan Dari Kulit Udang Jerbung (Penaeus merguiensis De Man) Dan Udang Windu

(Penaeus monodon Fabricius). SITAWA : Jurnal Farmasi Sains dan Obat Tradisional 2(1):. DOI:10.62018/sitawa.v2i1.24.

Younes, I., Rinaudo, M. 2015. Chitin and chitosan preparation from marine sources. Structure, properties and applications. Marine Drugs. DOI:10.3390/md13031133.

Zamani Mazdeh, F., Salami, F., Niazi, F., Chalipour, A., Tamiji, Z., Amini, M., Salehifar, M., Hajimahmoodi, M. 2025. Comprehensive Analysis of Bioactive Compounds in Malt Beverages: A Chemometric Approach for Quality Control. Journal of Agricultural Science and Technology 27(3):. DOI:10.22034/jast.27.3.617.

Zhang, J., Zhang, S., Niu, J., Dong, Z., Xu, J., Cui, T., Lei, C. 2025. Direct synthesis of α-Carboxyl-ω-Hydroxyl polymers by catalyst and initiator in the same molecule. European Polymer Journal 223. DOI:10.1016/j.eurpolymj.2024.113656.